


Effect of POE-*g*-GMA on mechanical, rheological and thermal properties of poly(lactic acid)/poly(propylene carbonate) blends

Ye Zhou¹ · Jiao Wang¹ · Shen-Yang Cai¹ · Zhi-Gang Wang¹ · Nai-Wen Zhang² · Jie Ren¹ 

Received: 28 August 2017 / Revised: 9 March 2018 / Accepted: 17 April 2018 /

Published online: 21 April 2018

© Springer-Verlag GmbH Germany, part of Springer Nature 2018

Abstract Glycidyl methacrylate (GMA) functionalized polyolefin elastomers (POE) (POE-*g*-GMA), which was a reactive processing agent, was melt-blended with poly(lactic acid) (PLA) and poly(propylene carbonate) (PPC) by twin-screw extrusion. The mechanical property results showed that with the addition of POE-*g*-GMA, the elongation at break and impact toughness of PLA/PPC blends increased while the tensile strength decreased. Dynamic thermomechanical analysis (DMA) and scanning electron microscope (SEM) results indicated that PLA/POE-*g*-GMA/PPC blends were partly miscible and the addition of POE-*g*-GMA improved the compatibility of blends. The higher T_{cs} and lower T_{ms} of PLA/POE-*g*-GMA/PPC blends showed a depressed crystalline ability of PLA caused by the decreased chain mobility according to the differential scanning calorimetry results and the thermal stability of PLA/POE-*g*-GMA/PPC blends was enhanced. Rheological results revealed that the addition of POE-*g*-GMA made the storage modulus (G'), loss modulus (G'') and complex viscosity of the blends increase, the melt strength also improved. These findings contributed to the biodegradable materials application for designing and manufacturing PLA film.

Keywords Poly(lactic acid) · Poly(propylene carbonate) · Mechanical properties · Rheological properties

✉ Jie Ren
renjie6598@163.com

¹ Institute of Nano and Bio-Polymeric Materials, Key Laboratory of Advanced Civil Engineering Materials (Tongji University), Ministry of Education, School of Material Science and Engineering, Tongji University, Shanghai 201804, China

² Shanghai Tong-Jie-Liang Biomaterials Co. Ltd., Shanghai 200438, China

Introduction

Nowadays, people show great interest in the development of commercial products made of biodegradable and renewable materials because of the worldwide environmental concern and energy crisis [1, 2]. Poly(lactic acid) (PLA), a bio-based green thermoplastic derived from biomass (corn, cassava or sugar beets), can eventually be converted to carbon dioxide, water and humus [3, 4]. PLA has high biodegradability and good mechanical properties compared to many petroleum-based plastics. Unfortunately, the brittleness and low glass transition temperature of the neat PLA are the major drawbacks for its application. And they are also problems for film extrusion of neat PLA [5, 6]. Many efforts have been made to improve the toughness of PLA; it is a more practical and economical measure to melt and blend PLA with other bio-degradable polymers including poly(ϵ -caprolactone) (PCL) [7], poly(butylenes succinate) (PBS) [8], poly(butyl-ene adipate-*co*-terephthalate) (PBAT) [9], poly(3-hydroxybutyrate-*co*-3-hydroxyvalerate) (PHBV) [10] and so on. Poly(propylene carbonate) (PPC), derived from carbon dioxide (CO₂) and propylene oxide, is a kind of new thermoplastic and biodegradable polymer with excellent physical and chemical properties [11–13]. It has been studied that the elongation and toughness of PLA/PPC blends increased dramatically with the increase of PPC content. However, many researchers also find that binary blends of PLA/PPC are partially miscible. Yan et al. [14] found that there was no evident phase separation when the content of PPC was less than 30% under optical microscope. But when the content of PPC reached 40%, phase separation took place. Yu et al. [15] and Zhang's group [16] reported that the PLA/PPC blends clearly indicated two separate T_g between PLA and PPC in the differential scanning calorimetry (DSC) results because of the incompatibility. As a two-phase system, the incompatibility between PLA and PPC especially at interfaces is still an unfavorable factor. It is a useful way to add the compatibilizer to improve these shortcomings [17–19]. Some researchers find that random copolymer or homopolymer can effectively improve the compatibility of incompatible blends and it can manipulate interface properties according to the selective localization of compatibilizer at the interface during the melting process [20–22]. Fu et al. [23] investigated the incorporation of maleic anhydride (MA) on the effect of PLA/PPC blends. They noted that, at low content such as 0.9% MA, the elongation at break of PLA/PPC blends reached 1355% and the strength hardly changed. However, higher MA content in the blends led to decrease in strength and further increase in toughness of the PLA/PPC blends indicating an obvious plasticizing effect. Further studies confirmed that a small amount of homopolymer poly(vinyl acetate) (PVAc) was able to enhance the mechanical properties of PLA/PPC blends, significantly improve the phase dispersion and increase the interfacial adhesion between PPC and PLA phases [24]. It is also considered that commercially available well-defined block or graft copolymer can be used as compatibilizer for immiscible polymer blends. However, to our knowledge, very limited papers have been reported so far to investigate the effect of well-defined block or graft copolymer on PLA/PPC blends.

In this paper, PPC was used to impart PLA with high toughness, moderate intensity and melt strength for film extrusion. On the other hand, glycidyl

fixed at 130 rpm. The test specimens were prepared from the over-dried extruded blends using an injection-molding machine (JETMASTER JN55-E) at 175 °C.

Mechanical properties

Tensile tests were conducted by using a CMT5105 electromechanical universal testing machine (Sans Group Company) adapted to the standard GB/T1040-2006. The crosshead speed was 50 mm min⁻¹.

Izod notched impact tests were conducted using a XCI-50 impact tester (Sans Group Company) adapted to the standard ISO GB/T1843-2008. Tests were done on specimens of 80 mm × 10 mm × 4 mm and a pendulum of 4 J. Five replicates were tested for each sample to get an average value.

Dynamic mechanical properties (DMA)

Dynamic mechanical properties (DMA) were characterized with a TA Instruments Q800 dynamic mechanical analyzer (USA) in a film-tension mode at a frequency of 1 Hz. The temperature ranged from – 10 to 90 °C at a heating rate of 3 °C min⁻¹. And the samples were 60 mm × 10 mm × 2 mm.

Scanning electron microscopy (SEM)

The morphologies of tensile fractured surfaces were observed by an SEM (HTTACHI S-2360N) at room temperature. For the tensile fractured specimens, they were sputter-coated with a thin layer of gold before examination.

Fourier transform infrared spectroscopy (FTIR)

The samples were compression-molded into films at 180 °C with a thickness of 50–100 μm, and the extracted samples were further analyzed by FTIR. ATR-IR technique was performed on a BRUKER Vertex 70 FTIR spectrometer at a resolution of 4 cm⁻¹ for 32 scans.

Differential scanning calorimetry (DSC)

The melting and crystallization behaviors of the blends were measured by a Q100 DSC analyzer (TA, USA) NETZSCH MDSC-Q100 DSC. The samples (about 3–5 mg) were first heated carried out from 25 to 200 °C at a rate of 20 °C min⁻¹ in nitrogen atmosphere. Then they were kept at 200 °C for 3 min to eliminate the previous heat history. Subsequently, the samples were cooled to 0 °C at the rate of 20 °C min⁻¹. The second heating processing was carried out from 0 to 220 °C at the rate of 10 °C min⁻¹.

Thermogravimetric analysis (TGA)

Thermogravimetric analysis (TGA) was performed under flowing air (80 ml min^{-1}) on a Q100 thermogravimetric analyzer (Tainstsh, USA) at a heating rate of $20 \text{ }^\circ\text{C min}^{-1}$. About 5 mg of samples, placed in a TGA pan, were heated from ambient temperature to $600 \text{ }^\circ\text{C}$.

Advanced rheometric expansion system (ARES)

Rheological properties were implemented with an Advanced Rheometric Expansion System (ARES) rheometer (TA, USA) using 25 mm diameter and 1.2 mm thickness plates at $175 \text{ }^\circ\text{C}$. A dynamic frequency sweep test was performed to determine the dynamic properties of blends. The range of dynamic frequency sweep test was from 0.1 to 300 rad s^{-1} , with 1% strain for the blends and in the region of linear viscoelastic response (LVR).

Results and discussion

Mechanical properties

The mechanical properties of PLA/PPC and PLA/PPC/POE-g-GMA were measured by tensile test and impact test at room temperature and are summarized in Table 1. Figure 1a shows the stress–strain curves of PLA/PPC blends. It was noted that neat PLA exhibited yielding without stress and necking, and fails at a strain around 3.07%. With the addition of PPC, the binary PLA/PPC blends showed visible stress and necking. The strain at break increased from 3.07 to 228.85% with the increasing content of PPC (10–90%); however, the tensile strength decreased from 61.50

Table 1 Mechanical properties of PLA/PPC and PLA/POE-g-GMA/PPC blends

Sample	Impact strength (kJ m^{-2})	Tensile strength (MPa)	Elongation at break (%)
PLA	16.60 ± 0.42	61.50 ± 1.46	3.07 ± 0.46
PLA/PPC (90/10)	19.12 ± 0.72	56.83 ± 1.88	4.47 ± 0.21
PLA/PPC (70/30)	16.15 ± 0.78	47.39 ± 2.57	17.70 ± 1.55
PLA/PPC (50/50)	13.72 ± 0.48	37.26 ± 2.82	43.20 ± 3.14
PLA/PPC (30/70)	12.35 ± 1.04	24.34 ± 1.61	174.12 ± 5.72
PLA/PPC (10/90)	10.22 ± 0.92	20.32 ± 2.50	228.85 ± 4.85
PLA/POE-g-GMA/PPC (30/1/69)	15.26 ± 0.72	16.60 ± 0.72	173.90 ± 8.56
PLA/POE-g-GMA/PPC (30/3/67)	23.47 ± 1.03	17.58 ± 1.03	205.12 ± 6.55
PLA/POE-g-GMA/PPC (30/5/65)	29.86 ± 0.86	18.69 ± 1.48	221.02 ± 4.14
PLA/POE-g-GMA/PPC (30/7/63)	25.18 ± 1.74	17.35 ± 1.24	212.46 ± 8.22

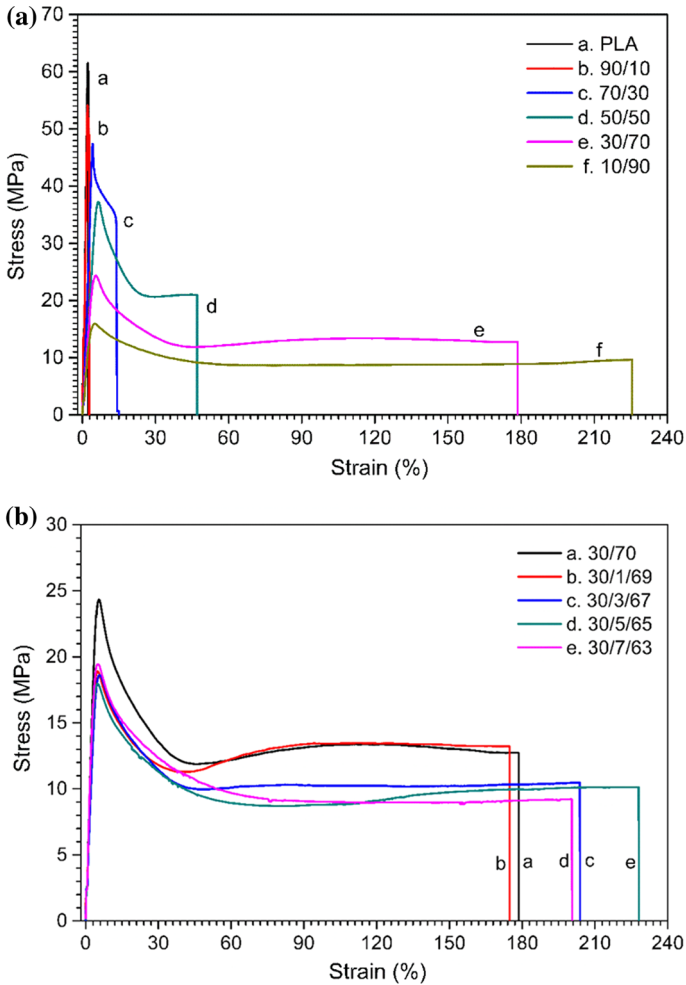


Fig. 1 Stress-strain curves for **a** PLA/PPC blends; **b** PLA/PPC (30/70 wt%) blends in the presence of POE-*g*-GMA

to 20.32 MPa. As we know, PLA materials require high toughness, moderate intensity and melt strength for film extrusion, so in this work, PLA/PPC (30/70) blends were chosen for further investigation with the addition of POE-*g*-GMA. As shown in Fig. 1b, the elongation at break was obviously improved in the presence of POE-*g*-GMA compared to before.

As shown in Fig. 2a, the tensile strength of the PLA/POE-*g*-GMA/PPC blend decreased when 1% POE-*g*-GMA was added, in comparison with the PLA/PPC binary blend. However, the tensile strength can be slightly increased from 16.60 to 18.69 MPa with the further addition of POE-*g*-GMA. From the Fig. 2b, we can also find that the elongations at break also increased when POE-*g*-GMA increased from 0 to 5%. These results indicated that POE effectively improves the

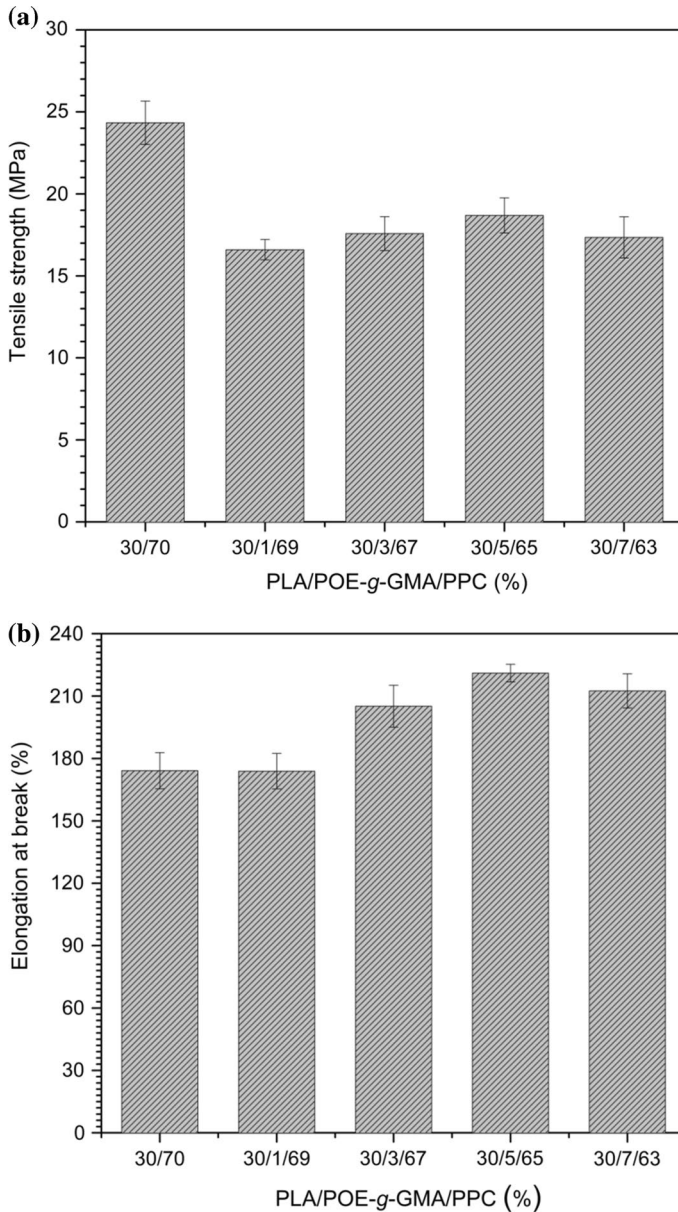


Fig. 2 **a** Tensile strength of PLA/PPC/POE-g-GMA blends; **b** elongation at break of PLA/PPC/POE-g-GMA blends

toughness of the polymer blends. Further addition of POE-g-GMA (7%) beyond the optimum amount (5%) had the opposite effect on tensile strength and ultimate strain as embrittlement sets in. This result agreed with that of literature [25].

Figure 3 gives the impact toughness of the blends. It is interesting to note that the toughness of blends exhibited the same tendency as the elongation at break. The impact strength enhanced dramatically from 15.26 to 29.86 kJ m⁻² when POE-*g*-GMA content increased from 0 to 5%, and decreased to 25.18 kJ m⁻² with further increasing POE-*g*-GMA content to 7%. All above results revealed that the compatibility between PLA and PPC was greatly improved by POE-*g*-GMA, indicating that a reaction took place between the epoxy groups of POE-*g*-GMA and carboxyl or hydroxyl groups of PLA/PPC. Thus, excess epoxy groups may lead to cross-linking, which brought about saturated and evenly decreased of impact strength. The possible reaction of PLA, PPC, and POE-*g*-GMA showed in Scheme 1.

Dynamic mechanical analysis (DMA) properties

Typical $\tan \delta$ curves for PLA, PPC and PLA/PPC/POE-*g*-GMA blends are shown in Fig. 4. There are two glass transition temperatures (T_g): the lower one corresponding to the PPC phase and the higher one corresponding to the PLA. And T_{g1} and T_{g2} of all samples were summarized in Table 2. The T_g of pure PLA and pure PPC presents 75.1 and 26.1 °C, respectively. When 70% PPC was added to PLA, the T_g of PLA decreased while T_g of PPC increased. It is also noted that T_{g1} of PPC shifts from 25.4 to 37.6 °C and T_{g2} of PLA shifts from 65.6 to 69.5 °C with the increase of POE-*g*-GMA content (1–7%), respectively. This clearly indicates that POE-*g*-GMA reacted with PLA and PPC as a reactive substance resulting in higher molecular segments which limit the movement of the segment. From DMA results, we can

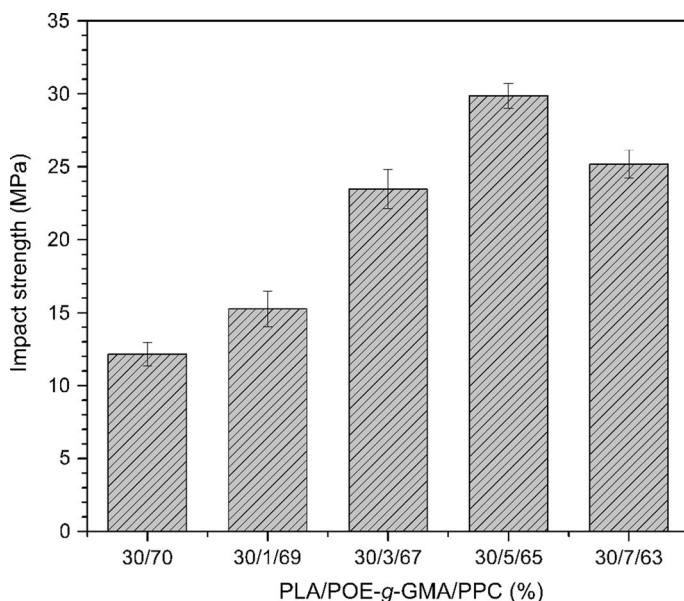


Fig. 3 Impact strength of PLA/POE-*g*-GMA/PPC blends

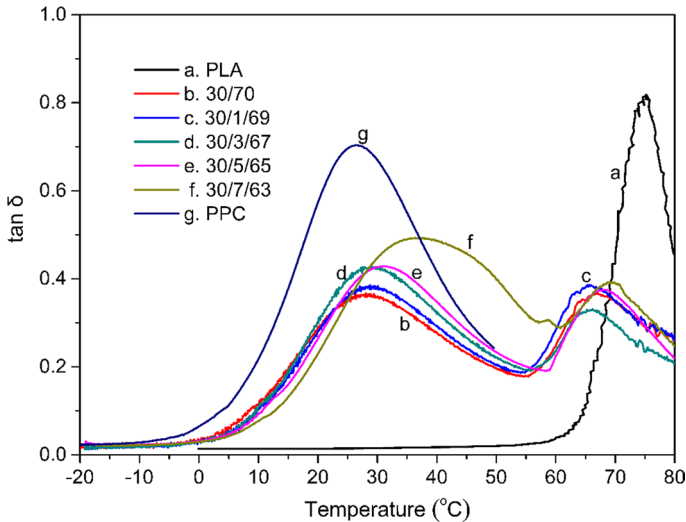


Fig. 4 $\tan \delta$ as a function of temperature for PLA/POE-*g*-GMA/PPC blends

Table 2 DMA results of PLA/POE-*g*-GMA/PPC blends

	PLA	PPC	30/70	30/1/69	30/3/67	30/5/65	30/7/63
T_{g_1}		25.4	26.8	28.3	29.5	31.5	37.6
T_{g_2}	73.9		65.6	65.4	66.2	67.4	69.5

conclude that the compatibility of PLA/PPC blends was improved with the addition of POE-*g*-GMA.

Morphological analysis by SEM

In order to further prove the enhanced compatibility by adding POE-*g*-GMA to PLA/PPC blends, the phase morphology of PPC/PLA and PLA/PPC/POE-*g*-GMA blends was investigated by SEM. The morphology of tensile specimens is presented in Fig. 5. Figure 5a clearly revealed that PLA/PPC (30/70) blends showed a kind of immiscible, namely, two-phase structure, as well as cavitation caused by de-bonding. This phenomenon indicated that the weak interfacial adhesion is associated with the incompatibility in PLA/PPC blends. The weak interface between PLA and PPC was also responsible for limited improvement in mechanical properties. For PLA/PPC/POE-*g*-GMA (30/65/5) blends, we could find that the phase interface became smooth, fuzzy and had no cavitation indicating that the interfacial adhesion between PLA and PPC was improved with the addition of POE-*g*-GMA, as shown in Fig. 5b. That was also the fact that the composites exhibited considerable ductile behavior and an appropriated improvement in toughness.

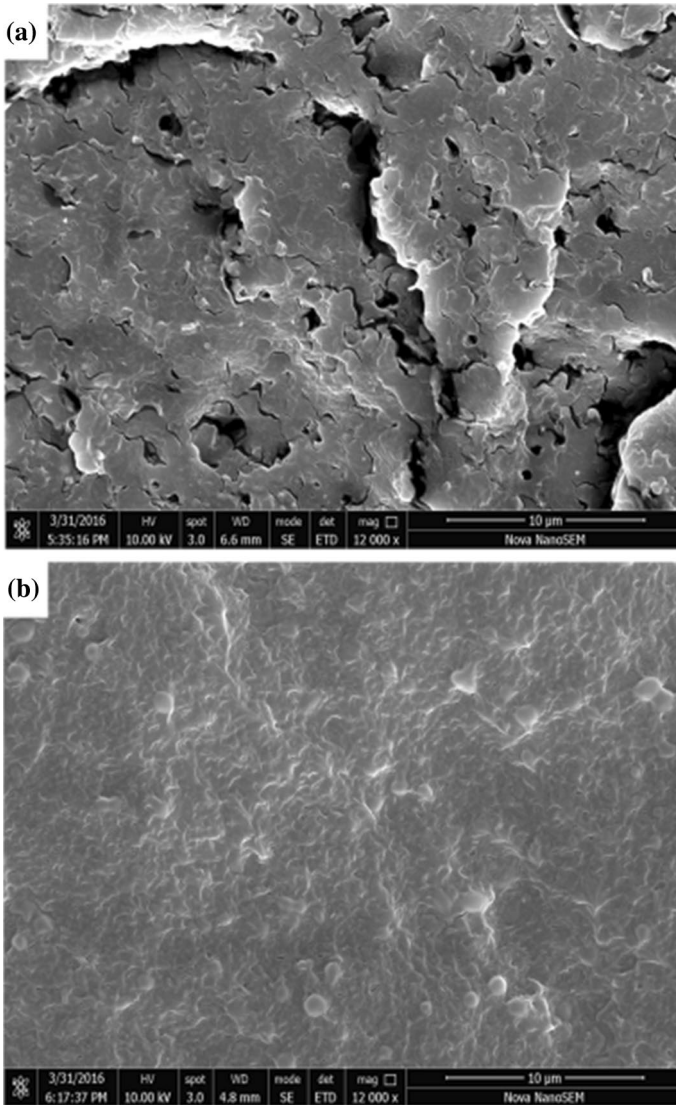


Fig. 5 Tensile-fractured surface morphology of the blends: **a** PLA/PPC (30/70); **b** PLA/POE-*g*-GMA/PPC (30/5/65)

FT-IR spectra analysis

The possible molecular mechanism for the interactions between the POE-*g*-GMA and the two matrix components (PPC and PLA) was analyzed with ATR-FTIR spectra (Fig. 6). The peak around 3400 cm^{-1} is very negligible due to the stretching vibration of O–H in end-hydroxyl groups and the peak around 2950 cm^{-1} is attributed to C–H bond stretching vibration. The band at 1748 cm^{-1} corresponds to

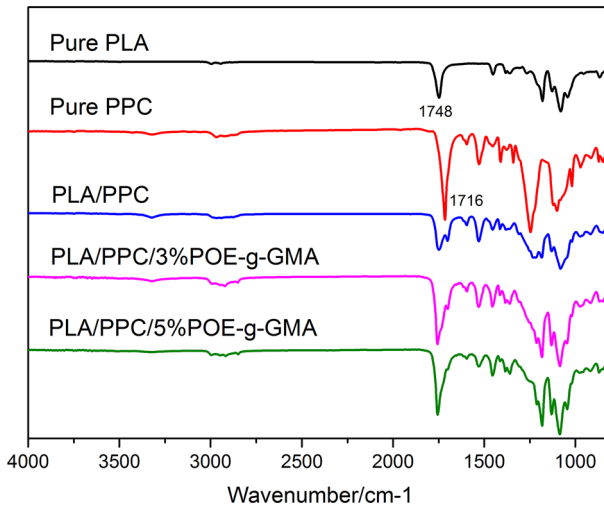


Fig. 6 FTIR spectra of PLA, PPC and the composites

the $\text{C}=\text{O}$ group of PLA and 1716 cm^{-1} corresponds to the $\text{C}=\text{O}$ group of PPC, respectively. Moreover, the peaks at 1716 cm^{-1} became weaker with the increase of POE-*g*-GMA, suggesting that POE-*g*-GMA was likely to react with the two components and improve the interaction between PPC and PLA molecules [26]. The $\text{O}-\text{C}-\text{O}$ stretching modes give rise to intense and complex multiple peaks from 1000 to 1200 cm^{-1} . These results indicated that the potential molecular mechanisms for the enhanced interaction may be the $\text{CH}_3\cdots\text{O}=\text{C}$ interaction between blends and the possible reaction of PLA, PPC, and POE-*g*-GMA.

Thermal analysis by DSC

In this study, as shown in Fig. 7 and Table 3, the melting and crystallization behavior of these blends were investigated. The second heating run was chosen as the DSC results for PLA/POE-*g*-GMA/PPC blends. The exothermic peaks could be regarded as the crystallization of PLA because of the amorphous nature of PPC and semi-crystalline nature of PLA. Comparing with DSC curves of different sample, there were some differences between the presence and absence of POE-*g*-GMA. As shown in Table 3, the incorporation of POE-*g*-GMA increased cold crystallization temperature (T_c) of PLA phase. As we know, the higher T_c of PLA indicated a depressed crystalline ability of PLA. The decreased cold crystallization ability of PLA phase may be attributed to the strong interaction between POE-*g*-GMA and PLA by hindering the movement and rearrangement of molecular chains. Correspondingly, the lower enthalpy of cold crystallization of the PLA also indicated lower degree of crystallization. For example, the ΔH_c values of the 30/70 PLA/PPC blends were 29.3 J g^{-1} , which decreased by about two times compared with that of PLA/POE-*g*-GMA/PPC (30/5/65) blends.

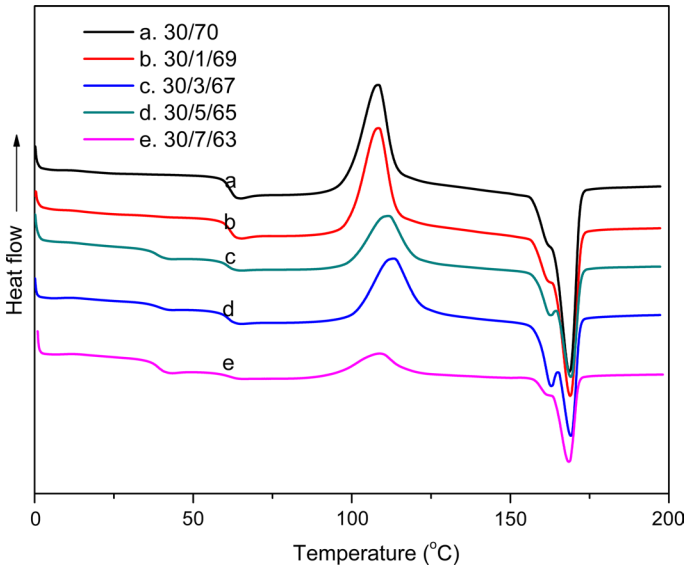


Fig. 7 DSC thermograms for PLA/POE-*g*-GMA/PPC blends during the second heating run

Table 3 DSC results of PLA/POE-*g*-GMA/PPC blends

POE- <i>g</i> -GMA content (%)	$T_c/^\circ\text{C}$	ΔH_c (J g^{-1})	$T_{m1}/^\circ\text{C}$	$T_{m2}/^\circ\text{C}$	ΔH_m (J g^{-1})
0	107.9	29.3	162.3	168.7	35.8
1	108.3	28.6	162.6	168.2	33.3
3	112.9	19.5	162.7	168.6	29.3
5	111.7	15.9	162.3	167.0	23.6
7	109.8	9.5	162.6	166.8	14.5

Furthermore, the PLA/PPC blends with or without POE-*g*-GMA displayed two melting peaks. The reason why two melting peaks originated was that some less perfect crystals gained enough time to be melted and reorganized into crystals with higher structural perfection at a relatively slow heating rate, and re-melted at higher temperature [27]. For PLA/POE-*g*-GMA/PPC blends, we can find that the second melting temperature (T_{m2}) slightly decreased with the increasing of POE-*g*-GMA; however, T_{m1} kept almost constant. The results could be explained as above results that the crystallization of perfect PLA crystalline is hindered by high molecular weight component and entangled macromolecules due to the reactions between POE-*g*-GMA and polymers.

Thermal stability by TGA

Figure 8 shows the TGA curves and DTG curves for PLA and its composites. From the results shown in Fig. 8a, it is found that PLA underwent a one-stage degradation

process which started decomposing around 321 °C ($T_{5\%}$) and almost no residue was left when heated to 400 °C. The thermal decomposition of PLA is a very complicated process that involves different mechanisms. At low temperatures, PLA degradation is based on the loss of end groups from the main chain (backbiting ester

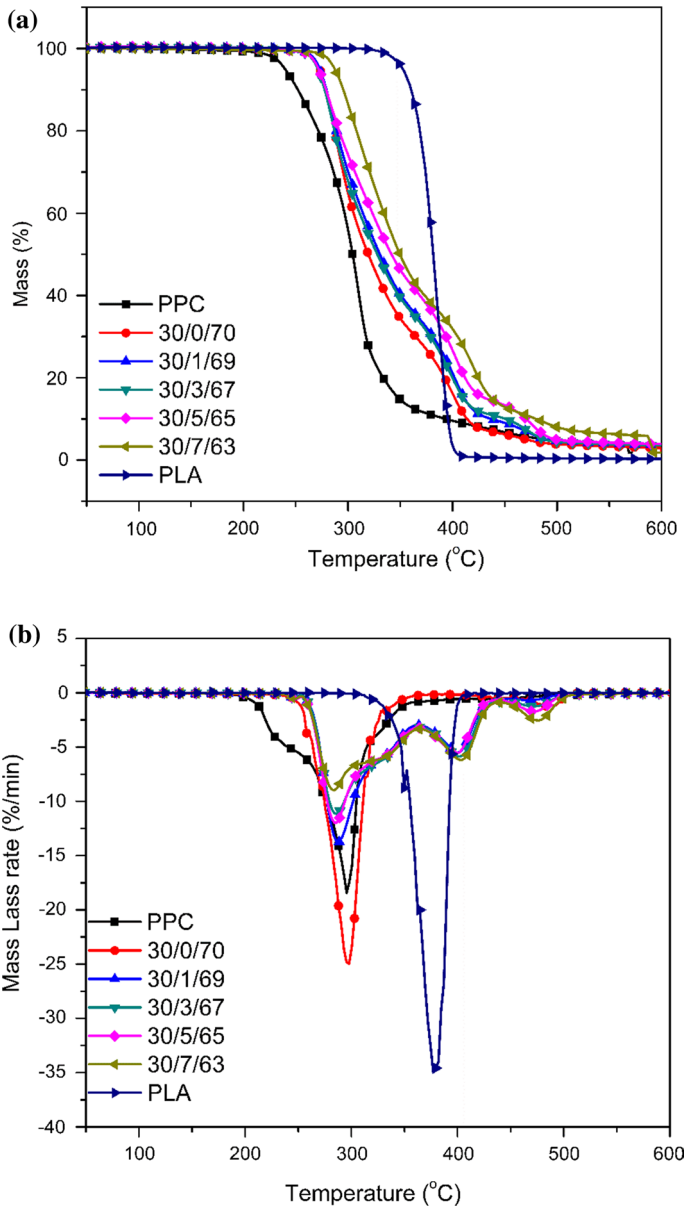


Fig. 8 **a** TGA curves and **b** DTG curves of PLA, PLA/PPC, PLA/POE-g-GMA/PPC blends under nitrogen

interchange) or ester change in intra- or intermolecular to form oligomers or cyclic oligomers. During decomposition, a lot of gaseous products are generated, such as cyclic oligomers, lactide, acetaldehyde, carbon monoxide and carbon dioxide. Degradation of plain PPC starts at quite low temperatures but fully decomposed around 570 °C. The addition of 70% PPC induced a shift of the degradation range of the blends to lower temperatures which greatly decreased the onset ($T_{5\%}$) and temperature at 50% mass loss ($T_{50\%}$) of neat PLA by 49 and 62 °C, respectively. Thermal decomposition of PPC occurs via random chain scission with evolution of CO₂ [28]. It is likely that the evolved gas interferes with thermal degradation mechanisms of PLA in the blends, accelerating it. As the same time, we can find that PLA/PPC (30/70) blends show a two-step degradation behavior in Fig. 8b. The first step corresponds to almost complete decomposition of the PPC matrix while the second one belongs to PLA. Compared to the pristine PLA without residual char, the PLA/PPC blends yielded 1.42 wt% char after the experiment. This behavior is mainly due to physical and chemical reactions promoted by transesterification of PLA and PPC.

When the POE-*g*-GMA was added in PLA/PPC blends, the main degradation process of the PLA/PPC blends fundamentally did not change but appeared a third step belonging to POE-*g*-GMA. It is interesting to note that after adding 1, 3, 5% POE-*g*-GMA, the onset ($T_{5\%}$) of PLA/PPC blends almost kept the same, however, temperature at 50% mass loss ($T_{50\%}$) of PLA/PPC blends increased by 8, 9 and 23 °C, respectively. When the POE-*g*-GMA is 7%, the onset ($T_{5\%}$) and temperature at 50% mass loss ($T_{50\%}$) of PLA/PPC blends increased by 16 and 29 °C. Compared to the PLA/PPC blends with 1.42 wt% residual char, the PLA/POE-*g*-GMA/PPC blends yielded 3.79 wt% char after the experiment. These phenomena demonstrated that the addition of POE-*g*-GMA enhanced thermal stability of PLA/PPC blends mainly due to physical and chemical reactions between the PLA and PPC promoted by POE-*g*-GMA (Table 4).

Rheological properties by ARES

As the addition of POE-*g*-GMA resulted in a finer phase structure (Fig. 5) and efficiently improved the mechanical properties of PLA/PPC blends, so ARES was carried out to investigate rheological properties of the blends with compatibilizer POE-*g*-GMA.

Figure 9a, b shows the storage modulus (G') and loss modulus (G'') curves of the PLA/POE-*g*-GMA/PPC blends. With the addition of POE-*g*-GMA, all the samples showed a typical increase in G' and G'' at nearly all frequencies. The higher absolute values of dynamic moduli indicated the formation of entanglement structures in PLA/PPC melts [29]. Now the higher storage modulus (G') and loss modulus (G'') of the melts clearly revealed a further entangled macromolecular chain. This may be due to the fact that POE-*g*-GMA is easy to entangle with PLA and PPC due to its long chain by the increase of POE-*g*-GMA content.

The complex viscosity (η^*) of PLA/POE-*g*-GMA/PPC blends was shown as Fig. 9c. It can be clearly seen that all samples displayed a shear-thinning tendency indicating a classical liquid-like behavior of the polymer melt. And the addition of

Table 4 Results of thermogravimetric analysis

Sample	$T_{5\%}$ (°C) ^a	$T_{50\%}$ (°C) ^b	T_{\max} (°C) ^c			CR _{exp} ^d
			Step 1	Step 2	Step 3	
PLA/POE- g-GMA/ PPC						
PLA	321	378	380	–	–	–
PPC	271	320	297	–	–	1.42
30/0/70	272	328	288	400	–	3.79
30/1/69	274	330	285	402	473	3.71
30/3/67	270	329	285	398	473	3.72
30/5/65	271	340	284	403	476	4.17
30/7/63	288	350	285	405	478	6.01

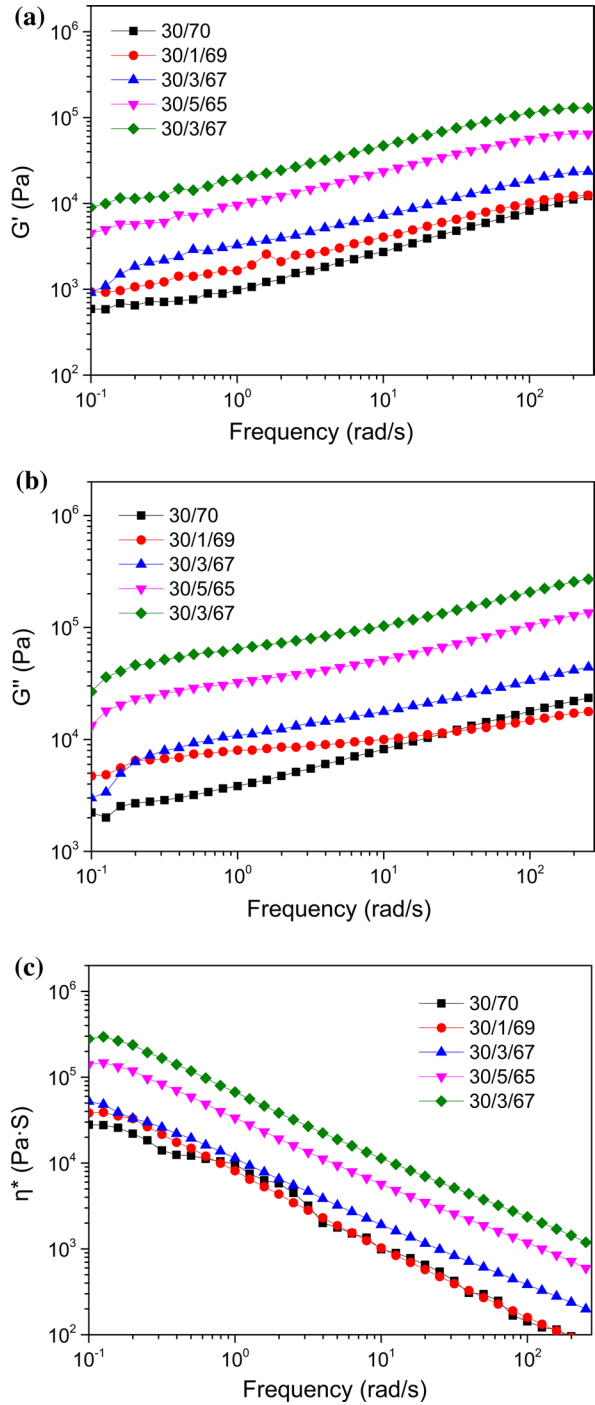
^aTemperature at 5% mass loss^bTemperature at 50% mass loss^cTemperature at maximum degradation rate^dThe experimental value of char residue at 600 °C

POE-*g*-GMA had a dramatic effect on the complex viscosity of the blends resulting in higher η^* at nearly all frequencies. The increasing complex viscosity of PLA/POE-*g*-GMA/PPC blends indicated that the reaction between POE-*g*-GMA and the PLA/PPC blends greatly increased the molecular interactions of the blend system and remarkably hindered the movement of molecular chains. Furthermore, the enhancement in complex viscosity of PLA/POE-*g*-GMA/PPC blends had been largely improved, which could be used in film extrusion.

Conclusions

The blends of PLA/PPC and PLA/PPC with POE-*g*-GMA as a reactive processing agent were successfully prepared by melt extrusion. The effect of POE-*g*-GMA on the mechanical properties, miscibility, phase morphology, crystallization behavior and rheology were investigated. With the addition of POE-*g*-GMA, the blends yielded with stress whitening and necking. And the strain-at-break of the PLA/POE-*g*-GMA/PPC blends and impact toughness was dramatically increased without severe loss in tensile strength. DMA results showed that PLA/POE-*g*-GMA/PPC blends were partially miscible. The T_g of PLA and PPC both shifted toward higher temperatures at the presence of POE-*g*-GMA due to the enhanced effect of POE-*g*-GMA on PLA/PPC blends. SEM results indicated that PLA/PPC blends transformed from two-phase structure to fuzzy, smooth phase interface revealing better miscibility of PLA/PPC blends with the addition of POE-*g*-GMA. Furthermore, the enhanced interfacial adhesion between PLA and PPC phases resulted in ductile behavior and the increasing toughness. ATR-FTIR study indicated the occurrence of the chemical reaction between PLA, PPC and POE-*g*-GMA, which accounted for the formation of a new copolymer. The higher T_{cs} and lower T_{ms} of PLA/POE-*g*-GMA/PPC blends showed a depressed crystalline ability of PLA caused by the decreased

Fig. 9 **a** Storage modulus (G'); **b** loss modulus (G''); **c** complex viscosity (η^*) versus frequency for PLA/POE-*g*-GMA/PPC blends



chain mobility. From the TGA results, the POE-*g*-GMA functions as a reactive agent to enhance the thermal stability of PLA/PPC blends. Rheological results revealed that the addition of POE-*g*-GMA made the storage modulus (G'), loss modulus (G'') and complex viscosity of the blends increase, and the melt strength also improved.

Acknowledgements The authors are grateful to the National High-Tech R&D Program of China (no. 2013AA032202), the National Natural Science Foundation of China (no. 51203118), the Shanghai Automotive Industry Science and Technology Development Foundation (Grant no. 1006), the Fundamental Research Funds for the Central Universities and the Open Funds for Characterization of Tongji University.

References

1. Van VK, Kiekens P (2002) Biopolymers: overview of several properties and consequences on their applications. *Polym Test* 21:433–442
2. Zhu DY, Guo JW, Chen SH, Pan LH (2015) Synthesis and performances of biodegradable copolymers of disodium *cis*-epoxysuccinate and 2,3-oxiranerethane sulfonic acid sodium used as non-phosphoric detergent builders. *Polym Bull* 72:93–102
3. Chen DK, Li JB, Ren J (2012) Biocomposites based on ramie fibers and poly(L-lactic acid) (PLLA): morphology and properties. *Polym Adv Technol* 23:198–207
4. Rodrigo GFC, Glaucia SB, Ribeiro C (2016) Nanocomposite fibers of poly(lactic acid)/titanium dioxide prepared by solution blow spinning. *Polym Bull* 73:2973–2985
5. Chen DK, Li JB, Ren J (2011) Influence of fiber surface-treatment on interfacial property of poly(L-lactic acid)/ramie fabric biocomposites under UV-irradiation hydrothermal aging. *Mater Chem Phys* 126:524–531
6. Bijarimi M, Ahmad S, Alam M (2016) Toughening effect of liquid natural rubber on the morphology and thermo-mechanical properties of the poly(lactic acid) ternary blend. *Polym Bull* 74:3301–3317
7. Harada M, Iida K, Okamoto K, Hayashi H, Hirano K (2008) Reactive compatibilization of biodegradable poly(lactic acid)/poly(epsilon-caprolactone) blends with reactive processing agents. *Polym Eng Sci* 48:1359–1368
8. Xie L, Xu H, Niu B, Ji X, Chen J, Li ZM, Hsiao BS, Zhong GJ (2014) Unprecedented access to strong and ductile poly(lactic acid) by introducing in situ nanofibrillar poly(butylene succinate) for green packaging. *Biomacromol* 15:4054–4064
9. Arruda LC, Magaton M, Ueki MM (2015) Influence of chain extender on mechanical, thermal and morphological properties of blown films of PLA/PBAT blends. *Polym Test* 43:27–37
10. Zembouai I, Kaci M, Bruzaud S, Dumazert L, Bourmaud A, Mahlous M, Lopez-Cuesta JM, Grohens Y (2016) Gamma irradiation effects on morphology and properties of PHBV/PLA blends in presence of compatibilizer and Cloisite 30B. *Polym Test* 49:29–37
11. Wu DD, Li W, Hao YP, Li ZL, Yang HL (2015) Mechanical properties, miscibility, thermal stability, and rheology of poly(propylene carbonate) and poly(ethylene-*co*-vinyl acetate) blends. *Polym Bull* 72:851–865
12. Du LC, Meng YZ, Wang SJ, Tjong SC (2004) Synthesis and degradation behavior of poly(propylene carbonate) derived from carbon dioxide and propylene oxide. *J Appl Polym Sci* 92:1840–1846
13. Kong JJ, Li ZL, Cao ZW, Han CY (2017) The excellent gas barrier properties and unique mechanical properties of poly(propylene carbonate)/organo-montmorillonite nanocomposites. *Polym Bull*. <https://doi.org/10.1007/s00289-017-2002-6>
14. Gao M, Ren ZJ, Yan SK, Sun JR, Chen XC (2012) An optical microscopy study on the phase structure of poly(L-lactide acid)/poly(propylene carbonate) blends. *J Phys Chem B* 116:9832–9837
15. Ma XF, Yu JG, Wang N (2006) Compatibility characterization of poly(lactic acid)/poly(propylene carbonate) blends. *J Polym Sci Pol Phys* 44:94–101
16. Liu HZ, Zhang JW (2011) Research progress in toughening modification of poly(lactic acid). *J Polym Sci Pol Phys* 49:1051–1083

17. Al-Itry R, Lamnawar K, Maazouz A (2014) Rheological, morphological, and interfacial properties of compatibilized PLA/PBAT blends. *Rheol Acta* 53:501–517
18. Zhang CL, Feng LF, Gu XP, Hoppe S, Hu GH (2007) Efficiency of graft copolymers as compatibilizers for immiscible polymer blends. *Polymer* 48:5940–5949
19. Hlavata D, Horak Z, Lednický F, Hromádková J, Pleska A, Zanevskii YV (2001) Compatibilization efficiency of styrene-butadiene multiblock copolymers in PS/PP blends. *J Polym Sci Pol Phys* 39:931–942
20. Xu YW, Thurber CM, Lodge TP, Hillmyer MA (2012) Synthesis and remarkable efficacy of model polyethylene-graft-poly(methyl methacrylate) copolymers as compatibilizers in polyethylene/poly(methyl methacrylate) blends. *Macromolecules* 45:9604–9610
21. Malik R, Hall CK, Genzer J (2011) Effect of copolymer compatibilizer sequence on the dynamics of phase separation of immiscible binary homopolymer blends. *Soft Matter* 7:10620–10630
22. Wang XY, Peng SW, Dong LS (2005) Effect of poly(vinyl acetate) (PVAc) on thermal behavior and mechanical properties of poly(3-hydroxybutyrate)/poly(propylene carbonate) (PHB/PPC) blends. *Colloid Polym Sci* 284:167–174
23. Yao M, Deng H, Mai F, Wang K, Zhang Q, Chen F, Fu Q (2011) Modification of poly(lactic acid)/poly(propylene carbonate) blends through melt compounding with maleic anhydride. *Express Polym Lett* 5:937–949
24. Gao J, Bai H, Zhang Q, Gao Y, Chen L, Fu Q (2012) Effect of homopolymer poly(vinyl acetate) on compatibility and mechanical properties of poly(propylene carbonate)/poly(lactic acid) blends. *Express Polym Lett* 6:860–870
25. Semba T, Kitagawa K, Ishiaku US, Hamada H (2006) The effect of crosslinking on the mechanical properties of polylactic acid/polycaprolactone blends. *J Appl Polym Sci* 101:1816–1825
26. Feng YL, Hu YX, Yin JH, Zhao GY, Jiang W (2013) High impact poly(lactic acid)/poly(ethylene octene) blends prepared by reactive blending. *Polym Eng Sci* 53:389–396
27. Zhao YQ, Cheung HY, Lau KT, Xu CL, Zhao DD, Li HL (2010) Silkworm silk/poly(lactic acid) biocomposites: dynamic mechanical, thermal and biodegradable properties. *Polym Degrad Stabil* 95:1978–1987
28. Li XH, Meng YZ, Zhu Q, Tjong SC (2003) Thermal decomposition characteristics of poly(propylene carbonate) using TG/IR and Py-GC/MS techniques. *Polym Degrad Stabil* 81:157–165
29. Zhang NW, Wang QF, Ren J, Wang L (2009) Preparation and properties of biodegradable poly(lactic acid)/poly(butylene adipate-co-terephthalate) blend with glycidyl methacrylate as reactive processing agent. *J Mater Sci* 44:250–256